Surface Subdivision Schemes Generated by Refinable Bivariate Spline Function Vectors

Charles K. Chui,* Qingtang Jiang

Department of Mathematics & Computer Science
University of Missouri–St. Louis
St. Louis, MO 63121

Abstract

The objective of this paper is to introduce a direct approach for generating local averaging rules for both the $\sqrt{3}$ and 1-to-4 vector subdivision schemes for computer-aided design of smooth surfaces. Our innovation is to directly construct refinable bivariate spline function vectors with minimum supports and highest approximation orders on the six-directional mesh, and to compute their refinement masks which give rise to the matrix-valued coefficient stencils for the surface subdivision schemes. Both the C^1-quadratic and C^2-cubic spaces are studied in some detail. In particular, we show that our C^2-cubic refinement mask for the 1-to-4 subdivision can be slightly modified to yield an adaptive version of Loop's surface subdivision scheme.

1. Introduction

In computer graphics, surface subdivision schemes of special interest are designed to generate (visually) continuous and smooth surfaces in an iterative manner, starting from some initial triangulations in the three dimensional space (3-D), with each iterative step consisting of two simple operations: generating a new set of points (called vertices) in 3-D, and connecting the vertices to give a new triangulation of higher resolution.

The two operations for each iterative step are governed by two rules. First a "topological rule" is needed to govern what new vertices are to be generated, and how they are to be connected to complete the triangulation when the vertices are in place. The second rule, called "local averaging rule", is designed to generate the new vertices by taking some weighted averages of the positions of the neighboring vertices from the previous iteration, as instructed by the topological rule. If the old vertices (i.e. vertices from the previous iteration) are not to be altered, the subdivision scheme is called an interpolatory subdivision scheme. On the other hand, if the local averaging rule is designed not

---

only to generate new vertices, but to change the locations of the old vertices as well, the subdivision scheme is called an approximation scheme.

The two rules, topological and local averaging rules, are specified in 2-D on a regular triangulation. For example, the 1-to-4 split topological rule, which asks for a new vertex between every two old vertices of each triangle (of the triangulation from the previous iteration) and specifies the connectivity instruction of these new vertices that splits the triangle into four sub-triangles, is described in the 2-D regular triangulation by connecting the midpoints of the three edges of each triangle. This is shown in Figures 1-2, where Fig.1A gives a 2-D regular triangulation that represents the 3-D surface in Fig.1B, while Fig.2A describes the 1-to-4 split topological rule. The actual positions of the new vertices in 3-D are governed by a local averaging rule. In Fig.2B, we describe such a rule by showing two coefficient stencils, one for the interior vertices and the other for vertices on the boundary, with values of the weights placed next to the old vertices, all shown in the 2-D representation. Fig.2C displays the finer triangulation after one iteration of the initial triangulation in Fig.1B. Since the initial vertices are not altered, this is an interpolatory subdivision scheme.

The 1-to-4 topological rule is most popular in the literature. For example, both the butterfly subdivision scheme [4] and Loop's scheme [16] engage the 1-to-4 topological rule. One of the main reasons for its popularity is that local averaging rules associated with it can be designed by considering the refinement (or two-scale) equation

$$\phi(\mathbf{x}) = \sum_{\mathbf{k}} p_{\mathbf{k}} \phi(2\mathbf{x} - \mathbf{k}), \quad \mathbf{x} \in \mathbb{R}^2, \tag{1}$$

with finite mask $\{p_{\mathbf{k}}\}$ that sum to 4, and that smoothness and polynomial preservation properties of the refinable function ϕ contribute to the smoothness of the limiting 3-D subdivision surfaces, when the values $p_{\mathbf{k}}$ from the refinement equation (1) are used as weights for the local averaging rule.

Recently, the so-called $\sqrt{3}$-subdivision scheme, introduced by Kobbelt [14] and Labsik-Greiner [15], and further studied in [12, 13, 17], engages a different topological rule, to be called $\sqrt{3}$-split rule in this paper for convenience. Here, again using a regular triangulation in 2-D as representation, the center of each triangle represents a new vertex in 3-D to be generated, and the connectivity instruction of the $\sqrt{3}$-split topological rule is to connect this new vertex to the three vertices of the triangle as well as to the three new vertices that are centers of the neighboring triangles. In addition, the old edges (i.e. edges from the previous iteration) are removed. In Figure 3, one iteration of the $\sqrt{3}$-split is shown in Fig.3B, and the second iteration is shown in Fig.3C. Observe that Fig.3C is a refinement of the triangulation in Fig.3A, and in fact, the dilation factor of the scaling of the triangulation in Fig.3A to yield the triangulation in Fig.3C is equal to 3. This is why the subdivision with this topological rule is called $\sqrt{3}$-subdivision.

To derive local averaging rules for the $\sqrt{3}$-subdivision, the refinement equation (1) is naturally modified to be

$$\phi(\mathbf{x}) = \sum_{k} p_{\mathbf{k}} \phi(A\mathbf{x} - \mathbf{k}), \quad \mathbf{x} \in \mathbb{R}^2, \tag{2}$$
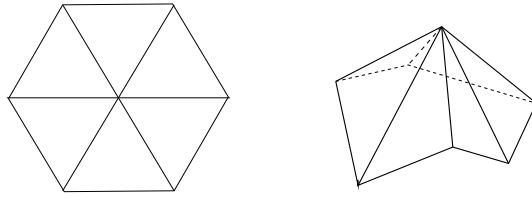
2

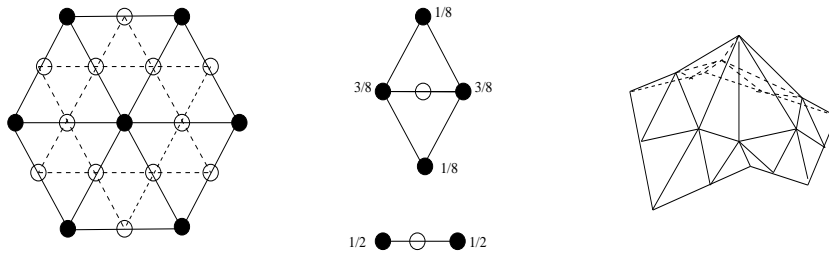Figure 1: Fig.1A: 2-D representation; Fig.1B: 3-D surface

Figure 2: Fig.2A: 1-to-4 split topological rule; Fig.2B: Local averaging rule; Fig.2C: 3-D surface
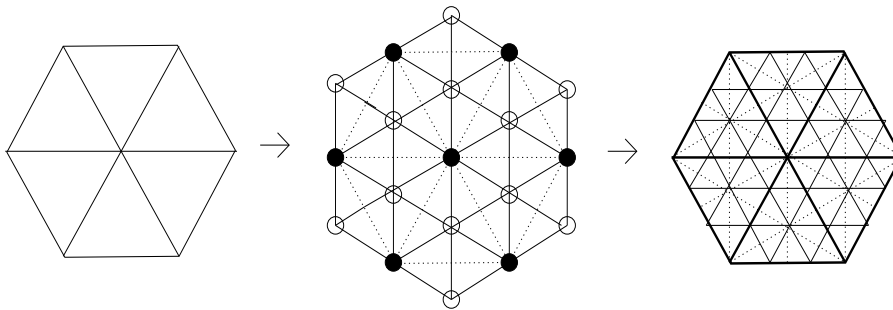

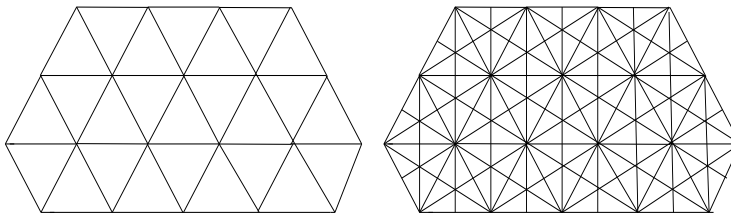Figure 3: (Fig.3A, Fig.3B, Fig.3C) Topological rule of $\sqrt{3}$-subdivision scheme

Figure 4: (Fig.4A, Fig.4B) Triangular meshes $\triangle_R^1$, $\triangle_R^3$

for some finite mask $\{p_\mathbf{k}\}$ to be constructed, where A is a 2×2 matrix with integer entries such that $|\det A| = 3$. Examples of such matrices A are:

$$A_0 = \begin{bmatrix} 1 & 2 \\ -2 & -1 \end{bmatrix}, \ A_1 = \begin{bmatrix} 2 & -1 \\ 1 & -2 \end{bmatrix}, \ A_2 = \begin{bmatrix} -1 & 2 \\ 1 & 1 \end{bmatrix}, \ A_3 = \begin{bmatrix} 1 & 1 \\ 2 & -1 \end{bmatrix}, \quad (3)$$

as well as $A_j^T, j = 0, \ldots, 3$. The so-called parametric approach [19, 18, 8, 5, 6] can be applied to solve the refinement equation (2). In fact, this is the approach used in [12, 13] with dilation matrix $A = A_0$ in (3). Again, smoothness and polynomial preservation are key ingredients for the smoothness of the 3-D subdivision surfaces.
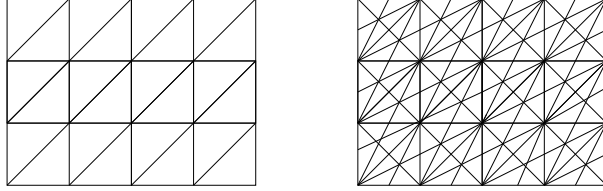

Figure 5: (Fig.5A, Fig.5B) 3- and 6-directional meshes $\triangle^1$, $\triangle^3$

In this paper, we consider a different approach. To present our point of view, let us first observe that if the edges from the previous iteration are not removed, then the triangulation in Fig.3B can be regarded as a triangulation achieved by using the 6-directional triangular mesh $\triangle_R^3$ shown in Fig.4B. In other words, the $\sqrt{3}$-split topological rule can be realized by considering some matrix dilation (and refinement) of $\triangle_R^3$. Indeed, the dilation matrix A_0 can be used for this purpose (see [12]). Of course the local averaging rules must be designed to introduce weights associated with the old vertices (from the previous iteration), which are vertices of the corresponding 3-directional (triangular) mesh $\triangle_R^1$ shown in Fig.4A. On the other hand, we believe that in studying the refinement equation (2) with dilation matrix A, the meshes $\triangle_R^1$ and $\triangle_R^3$ are not appropriate, since the translation operation in (2) is performed on the integer lattice $\mathbb{Z}^2$. For this reason, we choose the (topologically equivalent) 3-directional and 6-directional (triangular) meshes $\triangle^1$ and $\triangle^3$ shown in Figure 5, both of which are considered as triangulations of the entire x-y plane $\mathbb{R}^2$. To be more specific, the grid lines in $\triangle^1$ are $x = i, y = j, x - y = k$, and $\triangle^3$ is the refinement of $\triangle^1$ by introducing additional grid lines $x + y = \ell, x - 2y = m, 2x - y = n$ where $i, j, k, \ell, m, n \in \mathbb{Z}$. Hence, the $\sqrt{3}$-split topological rule described in Figure 3 is translated to the description in Figure 5 for the meshes $\triangle^1$ and $\triangle^3$. For the 6-directional mesh $\triangle^3$, we may choose the dilation matrices A_1, A_2 or A_3 (but not A_0), since they provide the "mesh refinability" property:

$$A_\ell \triangle^3 \subset \triangle^3, \quad \ell = 1, 2, 3, \quad (4)$$

in addition to satisfying the "grid partition condition":

$$\triangle^3 = \triangle^1 \cup A_\ell^{-1} \triangle^1, \quad \triangle^1 \cap A_\ell^{-1} \triangle^1 = \frac{1}{2}\mathbb{Z}^2, \quad \ell = 1, 2, 3. \quad (5)$$

4

This will be proved in the next section. In this regard, we remark that by considering

$$\triangle_-^1 = \{(x,y) : (-x,y) \in \triangle^1\}, \quad \triangle_-^3 = \{(x,y) : (-x,y) \in \triangle^3\},$$

all of the matrices A_0, A_1^T, A_2^T, and A_3^T provide the mesh refinability property and satisfy the grid partition condition, when $\triangle^1, \triangle^3$ in (4)–(5) are replaced by $\triangle_-^1, \triangle_-^3$.

To design the local averaging rules, the innovation we offer in this paper is to construct compactly supported bivariate splines $\phi_1, \cdots, \phi_n \in S_d^r(\triangle^3)$ directly, so that $\Phi = [\phi_1, \cdots, \phi_n]^T$ is a refinement function vector of some refinement equation:

$$\Phi(\mathbf{x}) = \sum_{\mathbf{k}} P_{\mathbf{k}} \Phi(A\mathbf{x} - \mathbf{k}) \tag{6}$$

with finite mask $\{P_{\mathbf{k}}\}$ of $n \times n$ matrices. The dilation matrices A of interest are $A = A_\ell$, $\ell = 1,2,3$, and $2I_2$, (but can be $3I_2$ as well). For $\sqrt{3}$-subdivision schemes, we only consider $A = A_1$ in this paper. Here, the notation $S_d^r(\triangle^3)$ denotes, as usual, the collection of all functions in $C^r(\mathbb{R}^2)$ whose restrictions on each triangle of the triangulation $\triangle^3$ are polynomials of total degree $\leq d$. The local averaging rule corresponding to (6) is then given by

$$\mathbf{v}_{\mathbf{j}}^{m+1} = \sum_{\mathbf{k}} \mathbf{v}_{\mathbf{k}}^m P_{\mathbf{j}-A\mathbf{k}}, \quad m = 0,1,\ldots, \tag{7}$$

where $\mathbf{v}_{\mathbf{k}}^m := [\mathbf{v}_{1,\mathbf{k}}^m, \cdots, \mathbf{v}_{n,\mathbf{k}}^m]$ is a "row-vector" whose ℓ^{th} component $\mathbf{v}_{\ell,\mathbf{k}}^m$ is a "point" in 3-D, for $\ell = 1,\ldots,n$. In particular, the first components $\mathbf{v}_{1,\mathbf{k}}^m$ will be used for the 3-D positions of the vertices of the triangulation resulting from the mth iterative step, with $\{\mathbf{v}_{1,\mathbf{k}}^0\}$ denoting the set of vertices of the initial triangulation, and $\{\mathbf{v}_{\ell,\mathbf{k}}^0\}, \ell = 2,\ldots,n$, providing the $3(n-1)$ parameters for shape control of the smooth subdivision surfaces. The local averaging rule (7), together with an appropriate topological rule ($\sqrt{3}$-split or 1-to-4 split) constitute what is called a vector subdivision scheme.

We mention that in a recent work [7], Han, Yu, and Piper also study the vector-valued refinement equation (6) for the design of vector subdivision schemes, but the method of derivation in [7] follows the parametric approach (see, particularly [6]) instead. It is interesting to point out that by choosing the parameters very cleverly, one may arrive at a bivariate spline solution of (6) indirectly. For example, for the dilation matrix $A = 2I_2$, the parametric solution in [7] is indeed in the space $S_2^1(\triangle^3)$, but for the dilation matrix $A = A_0^T$, the solution in [7] is not a piecewise polynomial function vector. On the other hand, again by the parametric approach, an unstable C^3 quartic box spline solution of the refinement equation (2) for the dilation matrix $A = A_0$ was obtained in [12] for the scalar-valued setting.

The direct refinable spline (function vector) approach we introduce in this paper can be used to develop vector subdivision schemes for designing surfaces with arbitrarily high order of smoothness by constructing refinable solutions from $S_d^r(\triangle^3)$ in general. We will derive complete results for the spaces $S_2^1(\triangle^3)$ and $S_3^2(\triangle^3)$ for both A_1 and $2I_2$. Of course, by replacing $\triangle^3$ with $\triangle_-^3$, the dilation matrices A_0, A_1^T, A_2^T, A_3^T can be used to yield analogous results for $\sqrt{3}$-subdivisions.

5

2. Preliminary results

Let A be any $s \times s$ matrix, $s \geq 2$, with integer entries and all eigenvalues λ satisfying $|\lambda| > 1$. For $n \geq 2$, let $\Phi = [\phi_1, \cdots, \phi_n]^T$, with $\phi_\ell \in L^2 := L^2(\mathbb{R}^s)$ and supp ϕ_ℓ bounded, $\ell = 1, \ldots, n$, satisfy the refinement equation (6) for some finite sequence $\{P_{\mathbf{k}}\}$ of $n \times n$ matrices, called the refinement mask of the refinement function vector Φ. Let

$$P(\mathbf{z}) := |\det A|^{-1} \sum_{\mathbf{k}} P_{\mathbf{k}} \mathbf{z}^{\mathbf{k}}$$

be the two-scale (matrix Laurent polynomial) symbol of Φ. Then $P(\mathbf{z})$ is said to possess the property of sum rules of order m (or $P \in SR_m$, for short), if there exists a trigonometric polynomial $\mathbf{t}(\omega)$ such that $\mathbf{t}(0) \neq 0$ and

$$D^{\mathbf{j}}(\mathbf{t}(A^T \omega) P(e^{-i\omega}))|_{\omega = 2\pi A^{-T} \omega_h} = \delta_{h,0} D^{\mathbf{j}} \mathbf{t}(0), \quad |\mathbf{j}| < m, \tag{8}$$

where ω_h, with $\omega_0 = 0$ and $0 \leq h \leq |\det A| - 1$, are the representers of $\mathbb{Z}^s / A^T \mathbb{Z}^s$. Then by setting

$$\mathbf{y}_\alpha := (-iD)^\alpha \mathbf{t}(0), \quad |\alpha| < m, \tag{9}$$

it follows that

$$\mathbf{x}^{\mathbf{j}} = \sum_{\mathbf{k}} \{ \sum_{\alpha \leq \mathbf{j}} \binom{\mathbf{j}}{\alpha} \mathbf{k}^{\mathbf{j} - \alpha} \mathbf{y}_\alpha \} \Phi(\mathbf{x} - \mathbf{k}), \quad \mathbf{x} \in \mathbb{R}^s, \ |\mathbf{j}| < m; \tag{10}$$

and hence, $P \in SR_m$ implies that $\Phi \in PP_m$, meaning that all polynomials of total degree $m - 1$ can be reproduced locally by integer translates of Φ (see the survey paper [10] and the references therein). Set

$$G_\Phi(\omega) := \sum_{\mathbf{k} \in \mathbb{Z}^s} \widehat{\Phi}(\omega + 2\mathbf{k}\pi) \widehat{\Phi}(\omega + 2\mathbf{k}\pi)^*.$$

It was shown in [9] that under the assumption $G_\Phi(0) > 0$ (i.e. $G_\Phi(0)$ is positive definite), we have $\Phi \in PP_m$ if and only if Φ has L^2-approximation order m. Finally, we also mention that $\{\phi_\ell(\cdot - \mathbf{k}) : \mathbf{k} \in \mathbb{Z}^s, \ell = 1, \ldots, n\}$ is a Riesz basis of the L^2-closure of its linear span if and only if $G_\Phi(\omega) > 0$ for all ω.

Let us now consider $s = 2$ and return to prove that the dilation matrices $A = A_\ell, \ell = 1, 2, 3$ in (3) satisfy (4) and (5).

Lemma 1. *The matrices A_1, A_2, A_3 provide the mesh refinability property (4) and satisfy the grid partition condition (5).*

Proof. We only provide the proof for A_1, since the proof for A_2 and A_3 is similar. That A_1 satisfies (5) is easy to verify (see Figure 6). The inclusion property (4) then follows from (5) and the fact that $A_1^{-2} \triangle^1 = \frac{1}{3} \triangle^1$, since

$$
\begin{aligned}
\triangle^3 &= \triangle^1 \cup (A_1^{-1} \triangle^1) \subset (\frac{1}{3} \triangle^1) \cup (A_1^{-1} \triangle^1) \\
&= (A_1^{-2} \triangle^1) \cup (A_1^{-1} \triangle^1) = A_1^{-1}((A_1^{-1} \triangle^1) \cup \triangle^1) = A_1^{-1} \triangle^3.
\end{aligned} \tag{11}
$$
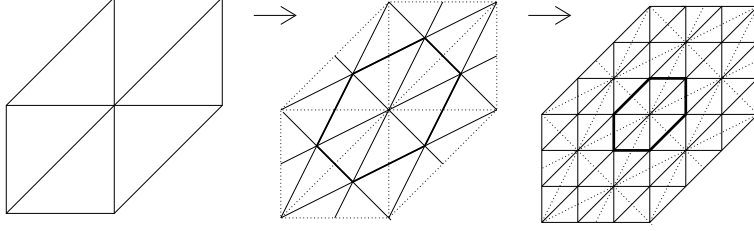
Figure 6: $\triangle^1 \to A_1^{-1}\triangle^1 \to A_1^{-2}\triangle^1 = \frac{1}{3}\triangle^1$

3. Local averaging rules for $\sqrt{3}$-subdivision schemes

Two local averaging rules are derived in this section for $\sqrt{3}$-subdivisions, one being interpolatory and the other approximation. The interpolatory subdivision scheme is a result of some refinable Hermite interpolating basis of $S_2^1(\triangle^3)$, and the approximation subdivision follows from the refinability of some basis functions in $S_3^2(\triangle^3)$.
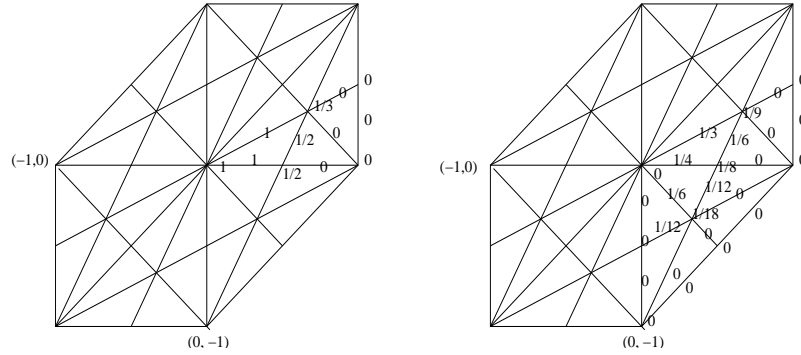
3.1. $\sqrt{3}$-subdivision based on $S_2^1(\triangle^3)$.

Figure 7: Supports and Bézier-nets for φ_1, φ_2 and $\varphi_3(x, y) = \varphi_2(y, x)$

A Hermite basis of $S_2^1(\triangle^3)$ was constructed in [3] (see the survey article [2] for details). It consists of integer shifts of three compactly supported splines $\varphi_1, \varphi_2, \varphi_3$ in $S_2^1(\triangle^3)$. The support and Bézier coefficients of φ_1 and φ_2 are shown in Figure 7, where in view of the symmetry properties:

$$\varphi_1(-x, -y) = \varphi_1(x, y), \quad \varphi_1(y, x) = \varphi_1(x, y), \quad \varphi_1(V\cdot) = \varphi_1, \quad \varphi_1(W\cdot) = \varphi_1, \quad (12)$$

$$\varphi_2(-x, -y) = -\varphi_2(x, y), \quad \varphi_2(V\cdot) = \varphi_2, \quad (13)$$

with $V = \begin{bmatrix} 1 & 0 \\ 1 & -1 \end{bmatrix}$, and $W = \begin{bmatrix} -1 & 1 \\ 0 & 1 \end{bmatrix}$, there is no need to display those Bézier coefficients not shown in the figure. Also, $\varphi_3(x, y) := \varphi_2(y, x)$. Set $\Phi^a := [\varphi_1, \varphi_2, \varphi_3]^T$. It is clear from the Bézier coefficients that Φ^a satisfies the Hermite interpolating property:

$$\left[\Phi^a, \frac{\partial}{\partial x}\Phi^a, \frac{\partial}{\partial y}\Phi^a\right](\mathbf{k}) = \delta_{\mathbf{k},0}I_3, \quad \mathbf{k} \in \mathbb{Z}^2. \quad (14)$$
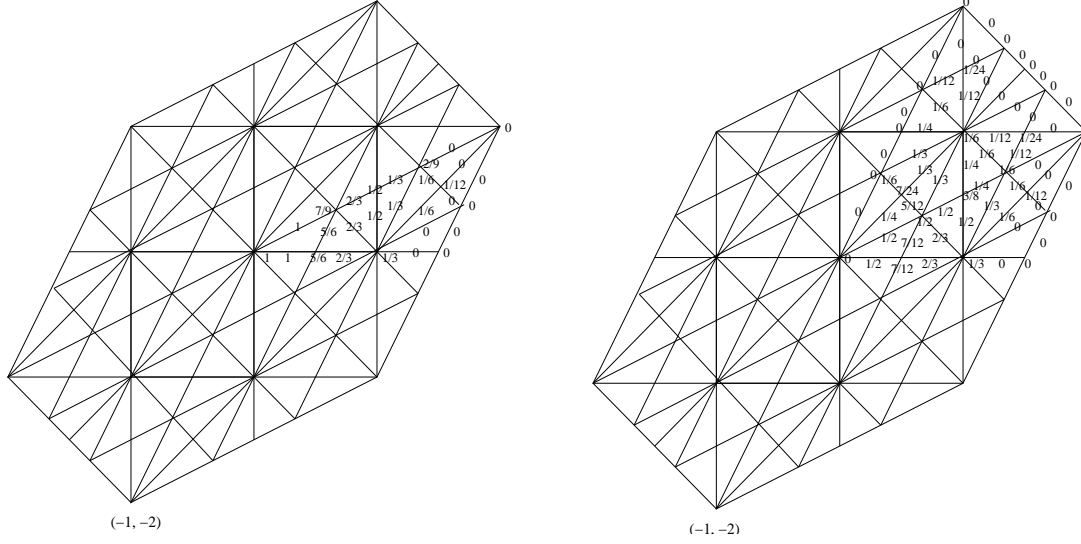
7

Figure 8: Supports and Bézier-nets for $\varphi_1(A_1^{-1}\cdot)$ and $3\varphi_2(A_1^{-1}\cdot)$

We have the following result.

Theorem 1. *Let $\varphi_1, \varphi_2, \varphi_3$ be the compactly supported bivariate spline functions in $S_2^1(\triangle^3)$ with Bézier coefficients shown in Figure 7. Then*

(i) *$\{\varphi_j(\cdot - \mathbf{k}) : \mathbf{k} \in \mathbb{Z}^2, j = 1, 2, 3\}$ is a Hermite (and hence Riesz) basis of $S_2^1(\triangle^3)$;*

(ii) *$\Phi^a = [\varphi_1, \varphi_2, \varphi_3]^T$ is refinable with dilation matrix A_1 and the refinement mask is given by*

$$P_{-1,-1} = \frac{1}{18} \begin{bmatrix} 6 & 12 & 12 \\ -1 & -2 & -2 \\ 1 & 2 & 2 \end{bmatrix}, \; P_{-1,0} = \frac{1}{18} \begin{bmatrix} 6 & 24 & -12 \\ -2 & -8 & 4 \\ -1 & -4 & 2 \end{bmatrix},$$

$$P_{0,-1} = \frac{1}{18} \begin{bmatrix} 6 & -12 & 24 \\ 1 & -2 & 4 \\ 2 & -4 & 8 \end{bmatrix}, P_{0,1} = \frac{1}{18} \begin{bmatrix} 6 & 12 & -24 \\ -1 & -2 & 4 \\ -2 & -4 & 8 \end{bmatrix}, \quad (15)$$

$$P_{1,0} = \frac{1}{18} \begin{bmatrix} 6 & -24 & 12 \\ 2 & -8 & 4 \\ 1 & -4 & 2 \end{bmatrix}, \; P_{1,1} = \frac{1}{18} \begin{bmatrix} 6 & -12 & -12 \\ 1 & -2 & -2 \\ -1 & 2 & 2 \end{bmatrix}, \; P_{0,0} = \frac{1}{3} \begin{bmatrix} 3 & 0 & 0 \\ 0 & 2 & -1 \\ 0 & 1 & -2 \end{bmatrix}.$$

(iii) *The two-scale symbol $P(z)$ satisfies $P \in SR_3$ and hence, Φ^a locally reproduces all bivariate quadratic polynomials; and*

(iv) *Φ^a has L^2-approximation order 3.*

Proof. We remark that (i) and (iv) were established in [3], but for completeness, we give the proof of all the statements (i)–(iv) in the following.

8

Let M, N be arbitrary positive integers and $S_2^1(\triangle_{MN}^3)$ denote the restriction of $S_2^1(\triangle^3)$ on $[0, M+1] \times [0, N+1]$. Since $\triangle_{MN}^3$ consists of $6(M+N+1)$ crosscuts, it follows from the dimension formula in [1, Theorem 4.3] that $\dim S_2^1(\triangle_{MN}^3) = 3(M+2)(N+2)$. Hence, as already shown in [2], the number of $\varphi_j(\cdot - \mathbf{k}), j = 1, 2, 3$ and $\mathbf{k} \in \mathbb{Z}^2$, whose supports overlap with $[0, M+1] \times [0, N+1]$, agrees with $\dim S_2^1(\triangle_{MN}^3)$. Since the Hermite interpolating property (14) implies linear independence, and since M, N are arbitrary, the statement (i) is valid. (For the proof of Riesz basis as a consequence of linear independence, see [11]).

To prove (ii), we first observe that in view of (i) and the refinability property (4) of A_1, Φ^a is indeed refinable. To find the refinement mask $\{P_\mathbf{k}\}$ in (15), we first compute the Bézier representation of $\varphi_j(A_1^{-1}\cdot), j = 1, 2, 3$, on $\triangle^3$ as shown in Figure 8, by applying the C^2-smoothing formula in [1, Theorem 5.1], and then write down the linear equations of $\varphi_j(A_1^{-1}\cdot)$, formulated as (finite) linear combinations of $\varphi_\ell(\cdot - \mathbf{k})$, $\mathbf{k} \in \mathbb{Z}$, and evaluated at the Bézier points. The (unique) solution, arranged in 3×3 matrix formulation, gives the mask shown in (15).

To prove (iii), it is not difficult to show that $P \in SR_3$ by finding a vector-valued trigonometric polynomial $\mathbf{t}$ that satisfies (8) and (9), with

$$\mathbf{y}_{0,0} = [1, 0, 0], \ \mathbf{y}_{1,0} = [0, 1, 0], \ \mathbf{y}_{0,1} = [0, 0, 1], \ \mathbf{y}_{2,0} = \mathbf{y}_{1,1} = \mathbf{y}_{0,2} = [0, 0, 0],$$

and hence, Φ^a reproduces all quadratic monomials $1, x, y, x^2, xy, y^2$.

Finally, since the Hermite basis has linear independent integer shifts, it is a Riesz basis of $S_2^1(\triangle^3)$, so that $G_{\Phi^a}(\omega) > 0$ for all ω and, in particular, $G_{\Phi^a}(0) > 0$. Hence, the fact that $\Phi^a \in PP_3$, as shown in (iii), implies that Φ^a has L^2-approximation order 3. This completes the proof of the theorem.

To describe the local averaging rule as given by (7) with $|\det A_1| = 3$ and $P_\mathbf{k}$ shown in (15), we use the coefficient stencils shown in Figure 9, where the solid circles denote the old vertices (i.e. vertices from the previous iteration) and the hollow circles denote the new vertices. In particular, in Fig.9B, each old vertex is simply multiplied by $P_{0,0}$ from the right. Hence, recalling from (7) that the first components $\mathbf{v}_{1,\mathbf{j}}^{m+1}$ of $\mathbf{v}_\mathbf{j}^{m+1}$ specify the locations of the vertices after m^{th} iteration, we see, from

$$\mathbf{v}_\mathbf{j}^{m+1} = [\mathbf{v}_{1,A_1^{-1}\mathbf{j}}^m, \ \frac{2}{3}\mathbf{v}_{2,A_1^{-1}\mathbf{j}}^m + \frac{1}{3}\mathbf{v}_{3,A_1^{-1}\mathbf{j}}^m, \ -\frac{1}{3}\mathbf{v}_{2,A_1^{-1}\mathbf{j}}^m - \frac{2}{3}\mathbf{v}_{3,A_1^{-1}\mathbf{j}}^m], \quad \mathbf{j} \in A_1\mathbb{Z}^2,$$

that the old vertices are not altered in position. Hence, this local averaging rule gives an interpolatory $\sqrt{3}$-subdivision scheme. The new vertices in 3-D are obtained, by considering only the first components of the weighted averages as shown in Fig.9C and Fig.9D, namely:

$$\mathbf{v}_e^1 = \mathbf{v}_a^0 P_{1,0} + \mathbf{v}_b^0 P_{0,1} + \mathbf{v}_c^0 P_{-1,-1}, \quad \mathbf{v}_f^1 = \mathbf{v}_a^0 P_{1,1} + \mathbf{v}_d^0 P_{0,-1} + \mathbf{v}_c^0 P_{-1,0}$$

which depend on the orientation of the new vertices as described in Fig.9A.

To end this sub-section, we remark that since $A_1^2 = 3I_2, \Phi^a$ is also refinable with dilation matrix $3I_2$ and the two-scale symbol is given by

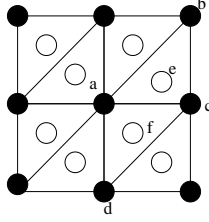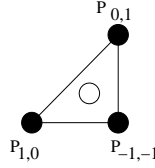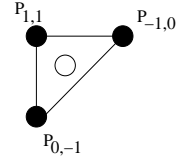$$P(e^{-iA_1^T\omega})P(e^{-i\omega}). \tag{16}$$

FIG.9.1 FIG.9.2 FIG.9.3 FIG.9.4

Figure 9: Coefficient stencils for the local averaging rule for the $\sqrt{3}$-subdivision

3.2. $\sqrt{3}$-**subdivision scheme based on** $S_3^2(\triangle^3)$. Again let $S_3^2(\triangle_{MN}^3)$ denote the restriction of $S_3^2(\triangle^3)$ on $[0, M+1] \times [0, N+1]$. Then the dimension formula in [1, Theorem 4.3] gives

$$\dim S_3^2(\triangle_{MN}^3) = 2MN + 6M + 6N + 16. \tag{17}$$

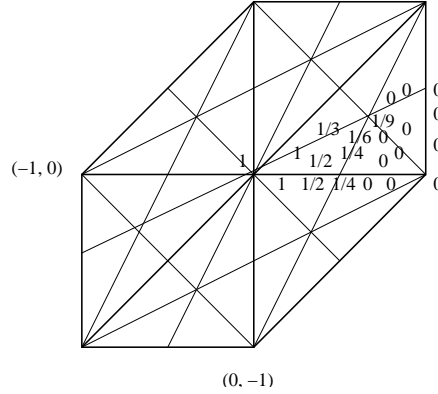Since the coefficient of MN is 2, we believe that $S_3^2(\triangle^3)$ is generated by integer shifts

Figure 10: Support and Bézier-nets for ϕ_1

of two compactly supported functions ϕ_1 and ϕ_2 in $S_3^2(\triangle^3)$. Based on the Bézier formulation of the univariate cardinal cubic B-spline (see [1, p. 13]), it is not difficult to construct the bivariate C^2 cubic spline ϕ_1 with minimum support, by applying the C^2-smoothing formula (see [1, Theorem 5.1]) and normalization condition $\phi_1(0) = 1$, as shown in Figure 10, where only a portion of the Bézier coefficients are displayed due to the symmetry property as described by (12) for a different basis function. For the other compactly supported basis function, we choose

$$\phi_2 = \phi_1(A_1^{-1}\cdot). \tag{18}$$

This choice of ϕ_2 is in some sense "optimal", since supp ϕ_2 contains 7 (interior) vertices of $\triangle^1$ and any ϕ with supp ϕ containing less than 7 vertices of $\triangle^1$ must be in the linear span of $\phi_1(\cdot - \mathbf{k})$, $\mathbf{k} \in \mathbb{Z}^2$. Hence, ϕ_2, as defined in (18), may be considered as a basis function in $S_3^2(\triangle^3)$ with the "second smallest" support.

10

As usual, set

$$V_j := \mathrm{clos}_{L^2}\langle \phi_1(A_1^j \cdot -\mathbf{k}) : \mathbf{k} \in \mathbb{Z}^2 \rangle, \tag{19}$$

and in view of (18), consider

$$U_j := V_j + V_{j-1}. \tag{20}$$

While it is not difficult to show that $\{V_j\}$ is not a nested sequence of subspaces, we will prove that $\{U_j\}$ is. Hence, $\Phi^b := [\phi_1, \phi_2]$ is indeed refinable. Unfortunately, inspite of their minimum supports, the number of $\phi_1(\cdot - \mathbf{j})$ and $\phi_2(\cdot - \mathbf{k})$, $\mathbf{k} \in \mathbb{Z}$, whose supports overlap with $[0, M+1] \times [0, N+1]$ is $2MN + 6M + 6N + 18$, which is larger than $\dim S_3^2(\triangle_{MN}^3)$ by 2. In other words, the integer shifts of ϕ_1 and ϕ_2 are governed probably by two linear dependence relations. To derive their linear dependence relationship, we introduce the function

$$g := \phi_1 - \frac{3}{2}\phi_2 \tag{21}$$

and establish the following.

Theorem 2. *Let $\phi_1 \in S_3^2(\triangle^3)$ with Bézier coefficients shown in Figure 10, and g be given by (21) with ϕ_2 defined by (18). Then g satisfies the following identities:*

$$G_1 := \sum_{\mathbf{k} \in \mathbf{Z}^2} \{g(\cdot - A_1\mathbf{k}) - g(\cdot - A_1\mathbf{k} + (1,0))\} = 0; \tag{22}$$

$$G_2 := \sum_{\mathbf{k} \in \mathbf{Z}^2} \{g(\cdot - A_1\mathbf{k}) - g(\cdot - A_1\mathbf{k} - (1,0))\} = 0. \tag{23}$$

Furthermore, these two independent identities describe the only linear dependence relationship between ϕ_1 and ϕ_2.

Proof. Let $\Omega_0 := \mathrm{supp}\, \phi_1$, as shown in Figure 10. It is clear that $\cup_{\mathbf{j} \in \mathbf{Z}^2}(\Omega_0 + A_1\mathbf{j}) = \mathbb{R}^2$. Hence, since $G_1(\cdot + A_1\mathbf{j}) = G_1$ for all $\mathbf{j} \in \mathbb{Z}^2$, it is sufficient to show that $G_1 = 0$ on Ω_0. This fact can be easily verified by evaluating G_1 at each Bézier point in Ω_0. The proof of (23) is similar.

To show that (22) and (23) govern the only linear dependence relationship, we set

$$\sum_{\mathbf{k} \in \mathbf{Z}^2} \{c_{\mathbf{k}}\phi_1(\mathbf{x} - \mathbf{k}) + d_{\mathbf{k}}\phi_2(\mathbf{x} - \mathbf{k})\} = 0, \quad \mathbf{x} \in [-1, 1] \times [-1, 1].$$

Then the coefficients $c_{\mathbf{k}}$ and $d_{\mathbf{k}}$ are uniquely determined by evaluating the equation at the Bézier points, giving the precise relationship of these coefficients, namely

$$c_{1,-1} = c_{-1,1} = c_{0,0} =: \alpha, \quad c_{0,-1} = c_{1,1} = c_{-1,0} =: \beta,$$

$$c_{-1,-1} = c_{0,1} = c_{1,0} = -(\alpha + \beta),$$

$$d_{0,0} = d_{-1,1} = d_{1,-1} = d_{-2,-1} = d_{-1,-2} = d_{2,1} = d_{1,2} = -\frac{3}{2}\alpha,$$

$$d_{-2,1} = d_{-1,0} = d_{0,-1} = d_{1,-2} = d_{-2,-2} = d_{0,2} = d_{1,1} = d_{2,0} = -\frac{3}{2}\beta,$$

$$d_{-1,2} = d_{0,1} = d_{1,0} = d_{2,-1} = d_{2,2} = d_{-2,0} = d_{-1,-1} = d_{0,-2} = \frac{3}{2}(\alpha + \beta),$$

11

where α and β are free parameters.

Theorem 3. *Let $\phi_1 \in S_3^2(\triangle^3)$, with Bézier coefficients shown in Figure 10, and ϕ_2 be defined by (18). Then*

(i) $S_3^2(\triangle^3) = \mathrm{clos}_{L^2}\langle\phi_j(\cdot - \mathbf{k}) : \mathbf{k} \in \mathbb{Z}^2, j = 1, 2\rangle$;

(ii) $\Phi^b = [\phi_1, \phi_2]^T$ *is refinable with dilation matrix A_1, and the two-scale symbol is given by*

$$P_{A_1}(\mathbf{z}) := \frac{1}{3} \left[\begin{array}{cc} 0 & 1 \\ \frac{1}{9} + \frac{2}{27}p(\mathbf{z}) + \frac{1}{27}p(\mathbf{z}^2) + \frac{1}{27}q(\mathbf{z}) & \frac{2}{3} + \frac{1}{3}p(\mathbf{z}) \end{array} \right],$$

where for $\mathbf{z} = (z_1, z_2)$, $\mathbf{z}^2 := (z_1^2, z_2^2)$, and

$$\begin{aligned}
p(\mathbf{z}) &:= z_1 + z_1^{-1} + z_2 + z_2^{-1} + z_1 z_2 + (z_1 z_2)^{-1}, \\
q(\mathbf{z}) &:= z_1^2 z_2 + z_1^{-2} z_2^{-1} + z_1 z_2^2 + z_1^{-1} z_2^{-2} + z_1 z_2^{-1} + z_1^{-1} z_2;
\end{aligned} \tag{24}$$

(iii) $P_{A_1} \in SR_4$, *and hence, Φ^b locally reproduces all bivariate cubic polynomials;*

(iv) Φ^b *has L^2-approximation order 4.*

Proof. The conclusion (i) follows from Theorem 2 and the fact that the number of $\phi_1(\cdot - \mathbf{j})$ and $\phi_2(\cdot - \mathbf{k})$ whose supports overlap with $[0, M + 1] \times [0, N + 1]$ equals to $\dim S_3^2(\triangle_{MN}) + 2$. Hence, in view of (4), Φ^b is refinable. To compute the refinement mask, and hence the two-scale symbol $P_{A_1}(\mathbf{z})$, we need to find all the Bézier coefficients of $\phi_j(A_1^{-1}\cdot), j = 1, 2$, on $\triangle^3$ by applying the C^3-smoothing formula in [1, Theorem 5.1] and solving the equation (7) at the Bézier points. That $P(\mathbf{z})$ has the property of SR_4 can be verified as in the proof of Theorem 1. Hence, $\Phi^b \in PP_4$ with $\mathbf{y}_\ell$ in (10) given by

$$\begin{aligned}
&\mathbf{y}_{0,0} = [1/6, \ 1/2], \ \mathbf{y}_{1,0} = \mathbf{y}_{0,1} = [0, \ 0], \ \mathbf{y}_{2,0} = \mathbf{y}_{0,2} = [1/18, \ -1/6], \\
&\mathbf{y}_{1,1} = [1/36, \ -1/12], \ \mathbf{y}_{3,0} = \mathbf{y}_{2,1} = \mathbf{y}_{1,2} = \mathbf{y}_{0,3} = [0, \ 0].
\end{aligned}$$

This completes the proof of (iii).

To prove (iv), let us first show that $G_{\Phi^b}(0) > 0$. Indeed, if this were false, then there exists a nontrivial pair (c_1, c_2) of constants for which $[c_1, c_2]G_{\Phi^b}(0)[c_1, c_2]^* = 0$, and this has the equivalent formulation $\sum_{\mathbf{k}} |c_1\hat{\phi}_1 + c_2\hat{\phi}_2|^2(2\mathbf{k}\pi) = 0$, so that $(c_1\hat{\phi}_1 + c_2\hat{\phi}_2)(2\mathbf{k}\pi) = 0$; and by the Poisson summation formula, we have $\sum_{\mathbf{k}}\{c_1\phi_1 + c_2\phi_2\}(\cdot - \mathbf{k}) = 0$. This contradicts with Theorem 2. Hence, we have $G_{\Phi^b}(0) > 0$. Recall that under this condition, order of local polynomial reproduction is equivalent to L^2-approximation order. Therefore, (iv) follows from (iii). This completes the proof of the theorem.

To describe the local averaging rule as given by (7) with $|\det A_1| = 3$ and $P_{\mathbf{k}}$ given by the matrix coefficients of $P_{A_1}(\mathbf{z})$, we introduce the notations

$$a := \left[\begin{array}{cc} 0 & 0 \\ 2/27 & 1/3 \end{array} \right], \quad b := \left[\begin{array}{cc} 0 & 0 \\ 1/27 & 0 \end{array} \right], \tag{25}$$

and observe that the nonzero $P_{\mathbf{k}}$'s are given by $P_{0,0} = \begin{bmatrix} 0 & 1 \\ 1/9 & 2/3 \end{bmatrix}$ and

$$
\begin{aligned}
P_{1,0} &= P_{-1,0} = P_{0,1} = P_{0,-1} = P_{1,1} = P_{-1,-1} = a, \\
P_{2,0} &= P_{-2,0} = P_{0,2} = P_{0,-2} = P_{2,2} = P_{-2,-2} = b, \\
P_{2,1} &= P_{-2,-1} = P_{1,2} = P_{-1,-2} = P_{1,-1} = P_{-1,1} = b.
\end{aligned}
\tag{26}
$$

In Figure 11, we display the coefficient stencils for this local averaging rule. Observe that the $\sqrt{3}$-subdivision scheme with this rule is not interpolatory in that the old vertices are altered by applying the coefficient stencil shown in the second figure of Figure 11.
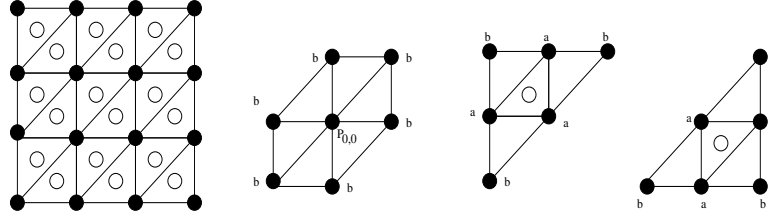

Figure 11: Coefficient stencils for the local averaging rule for the $\sqrt{3}$-subdivision

Remark 1. The basis function ϕ_1, with Bézier coefficients shown in Figure 10, is related to φ_2, φ_3, with Bézier coefficients shown in Figure 7, as follows:

$$
\frac{\partial \phi_1}{\partial x} = -12\varphi_2 + 6\varphi_3, \quad \frac{\partial \phi_1}{\partial y} = 6\varphi_2 - 12\varphi_3.
$$

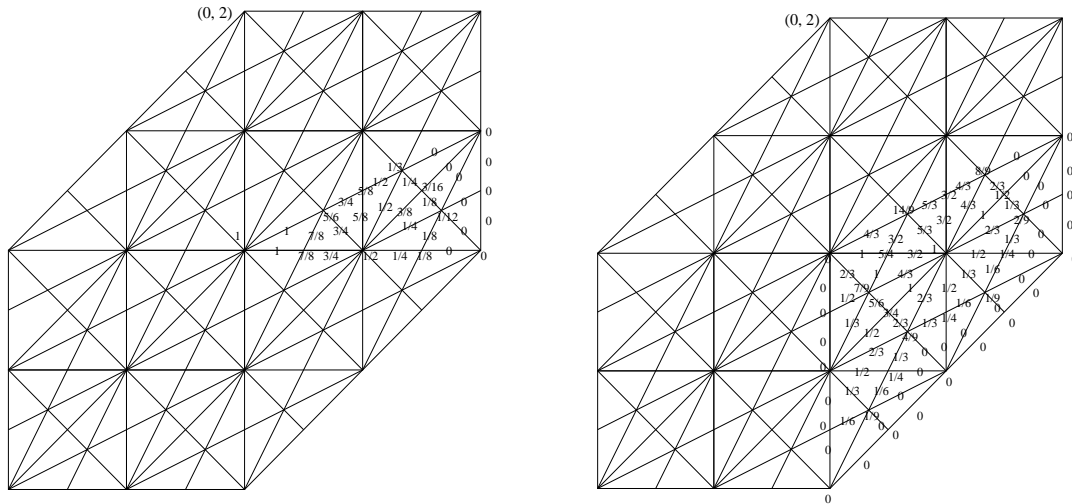## 4. Local averaging rules for 1-to-4 split subdivisions

Figure 12: Support and Bézier-nets for $\varphi_1(\cdot/2)$ and $8\varphi_2(\cdot/2)$

13

Since the matrix $A = 2I_2$ also has the mesh refinability property $2\triangle^3 \subset \triangle^3$, the theory derived in the previous section applies to 1-to-4 split subdivisions as well. In particular, for $S_2^1(\triangle^3)$ with $\Phi^a = [\varphi_1, \varphi_2, \varphi_3]$ as shown in Figure 7, it is not difficult to compute the refinement mask with dilation matrix $2I_2$ with

$$P_{0,0} = \mathrm{diag}(1, \tfrac{1}{2}, \tfrac{1}{2}), \; P_{1,1} = \frac{1}{8}\begin{bmatrix} 4 & -4 & -4 \\ 1 & 0 & -2 \\ 1 & -2 & 0 \end{bmatrix}, \; P_{1,0} = \frac{1}{8}\begin{bmatrix} 4 & -8 & 4 \\ 1 & -2 & 2 \\ 0 & 0 & 2 \end{bmatrix},$$

$$P_{-1,0} = \frac{1}{8}\begin{bmatrix} 4 & 8 & -4 \\ -1 & -2 & 2 \\ 0 & 0 & 2 \end{bmatrix}, \; P_{-1,-1} = \frac{1}{8}\begin{bmatrix} 4 & 4 & 4 \\ -1 & 0 & -2 \\ -1 & -2 & 0 \end{bmatrix}, \tag{27}$$

$$P_{0,1} = \frac{1}{8}\begin{bmatrix} 4 & 4 & -8 \\ 0 & 2 & 0 \\ 1 & 2 & -2 \end{bmatrix}, \; P_{0,-1} = \frac{1}{8}\begin{bmatrix} 4 & -4 & 8 \\ 0 & 2 & 0 \\ -1 & 2 & -2 \end{bmatrix},$$

by using the Bézier-nets of Φ^a and $\Phi^a(\frac{\cdot}{2})$ shown in Figure 7 and Figure 12, respectively. We note that this agrees with the refinement mask obtained in [7], using an indirect parametric approach. The local averaging rule for this subdivision is described by the coefficient stencils shown in Figure 13. Observe that this subdivision scheme is interpolatory.
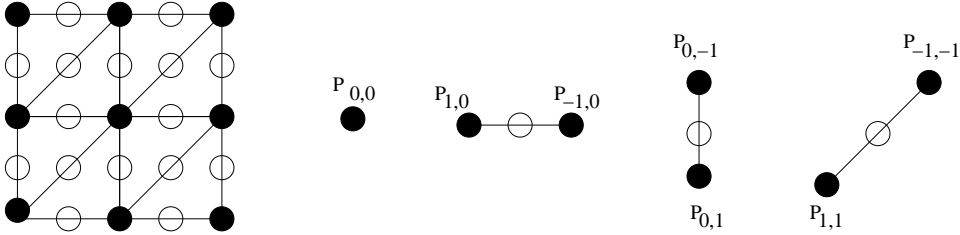

Figure 13: Coefficient stencils for the local averaging rule for the 1-to-4 subdivision

As for $S_3^2(\triangle^3)$, the bivariate spline function ϕ_1 shown in Figure 10 also gives rise to a refinable function vector $\Phi^b = [\phi_1, \phi_2]$ with dilation matrix $2I_2$, where $\phi_2 = \phi_1(A_1^{-1}\cdot)$ as defined in (18). The refinement mask is determined by the two-scale symbol

$$P_{2I_2}(\mathbf{z}) = \frac{1}{32}\begin{bmatrix} -1 + p(\mathbf{z}) & 9 \\ 1 + \frac{2}{3}p(\mathbf{z}) + \frac{1}{3}p(\mathbf{z}^2) + \frac{1}{3}q(\mathbf{z}) & 5 + 3p(\mathbf{z}) + q(\mathbf{z}) \end{bmatrix}, \tag{28}$$

where $p(\mathbf{z})$ and $q(\mathbf{z})$ are the Laurent polynomials given in (24). To describe the corresponding local averaging rule, we introduce the notations

$$c := \frac{1}{24}\begin{bmatrix} 3 & 0 \\ 2 & 9 \end{bmatrix}, \quad d := \frac{1}{24}\begin{bmatrix} 0 & 0 \\ 1 & 0 \end{bmatrix}, \quad e := \frac{1}{24}\begin{bmatrix} 0 & 0 \\ 1 & 3 \end{bmatrix}, \tag{29}$$

and observe that the nonzero coefficients of $P_{2I_2}(z)$ in (28) are given by $P_{0,0} = \frac{1}{8}\begin{bmatrix} -1 & 9 \\ 1 & 5 \end{bmatrix}$

and

$$P_{1,0} = P_{-1,0} = P_{0,1} = P_{0,-1} = P_{1,1} = P_{-1,-1} = c,$$

14

$$P_{2,0} = P_{-2,0} = P_{0,2} = P_{0,-2} = P_{2,2} = P_{-2,-2} = d, \tag{30}$$
$$P_{2,1} = P_{-2,-1} = P_{1,2} = P_{-1,-2} = P_{1,-1} = P_{-1,1} = e.$$

The coefficient stencils of this subdivision scheme are shown in Figure 14.

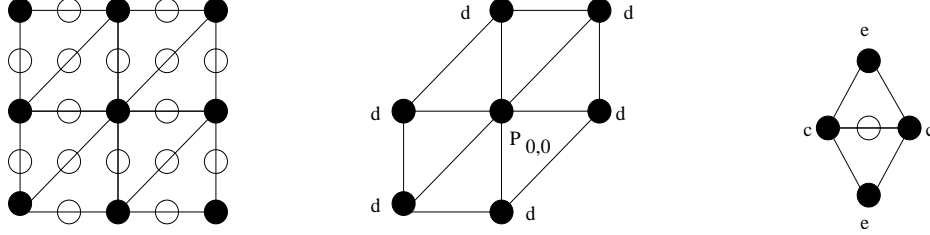

Figure 14: Coefficient stencils for the local averaging rule for the 1-to-4 subdivision

5. Further subdivision results based on $S_3^2(\triangle^3)$

In this section, we recapture and modify Loop's scheme by a simple modification of our 1-to-4 subdivision scheme based on $S_3^2(\triangle^3)$ and introduce two other local averaging rules, also based on $S_3^2(\triangle^3)$.
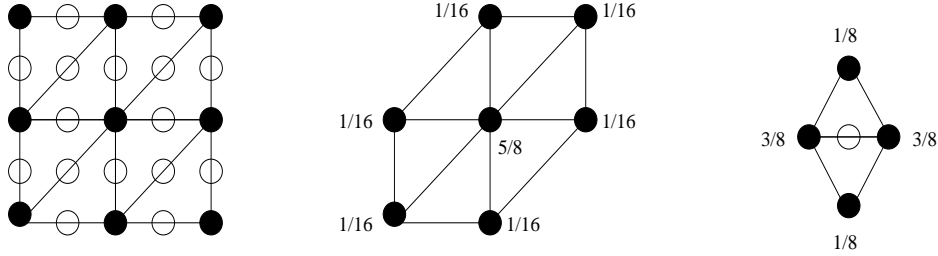

Figure 15: Coefficient stencils for the local averaging rule for the Loop's subdivision scheme

5.1. Loop's scheme with control parameters. Loop's scheme is a 1-to-4 split subdivision scheme with local averaging rule derived from the two-scale symbol

$$P_L(\mathbf{z}) := \frac{1}{32}\{5 + 3p(\mathbf{z}) + q(\mathbf{z}) + \frac{1}{2}p(\mathbf{z}^2)\}, \tag{31}$$

of the box-spline B_{222} on $\triangle^1$ where p and q are given in (24) (see [1, pp. 37–38] for a discussion of $B_{2r2r2r} \in S_{3r-2}^{2r-2}(\triangle^1)$, and in particular, $B_{222} \in S_4^2(\triangle^1)$, as the "only" compactly supported generator). The coefficient stencils for Loop's scheme are shown in Figure 15.

Now, return to the matrix-valued Laurent polynomial symbol P_{2I_2} in (28) of the refinement function vector $\Phi^b = [\phi_1, \phi_1(A_1^{-1}\cdot)]$, and consider its modification

$$\widetilde{\Phi} := U\Phi^b, \qquad U := \begin{bmatrix} \frac{1}{3} & 1 \\ \frac{1}{3} & -1 \end{bmatrix}. \tag{32}$$

15

It is clear that $\widetilde{\Phi}$ is again refinable with dilation matrix $2I_2$ and two-scale symbol

$$\widetilde{P}(\mathbf{z}) = UP_{2I_2}(\mathbf{z})U^{-1} = \begin{bmatrix} P_L(\mathbf{z}) & -\frac{3}{32} + \frac{1}{64}p(\mathbf{z}^2) \\ -\frac{3}{32} - \frac{1}{16}p(\mathbf{z}) - \frac{1}{64}p(\mathbf{z}^2) - \frac{1}{32}q(\mathbf{z}) & -\frac{1}{32} + \frac{1}{32}p(\mathbf{z}) - \frac{1}{64}p(\mathbf{z}^2) \end{bmatrix},$$
(33)

where the $(1,1)$-entry of $\widetilde{P}$ is the two-scale symbol P_L of B_{222}. Hence, if we consider the projection operator

$$Q : \mathbf{v_k} = [\mathbf{v_{1,k}}, \mathbf{v_{2,k}}] \to [\mathbf{v_{1,k}}, 0],$$

and set $S\{\mathbf{v_k^m}\} := \{\mathbf{v_j^{m+1}}\}$ in (7) (with $A = 2I_2$ and $\{P_\mathbf{k}\}$ being the matrix-valued coefficients of $\widetilde{P}(\mathbf{z})$ in (33)), then it follows that $(SQ)^m\{\mathbf{v_k^0}\}$ generates the same 3-D surface as Loop's scheme, by considering only the first component of $(SQ)^m\mathbf{v_k^0}$. Since $\mathbf{v_k^0} = [\mathbf{v_{1,k}^0}, \mathbf{v_{2,k}^0}]$, where $\{\mathbf{v_{1,k}^0}\}$ denotes the set of initial vertices, we gain a set of control parameters $\{\mathbf{v_{2,k}^0}\}$ for adaptive application of Loop's subdivision scheme.

5.2. More averaging rules based on $S_3^2(\triangle^3)$. The local averaging rules shown in Figure 11 and Figure 14 for the $\sqrt{3}$-split and 1-to-4 split topological rules, respectively, are based on the refinable function vector $[\phi_1, \phi_1(A_1^{-1}\cdot)]$ with $\phi_1 \in S_3^2(\triangle^3)$. Observe that the same $\phi_2 = \phi_1(A_1^{-1}\cdot)$ was used, even for the dilation matrix $2I_2$.

Let us now choose $\phi_1((2I_2)^{-1}\cdot) = \phi_1(\frac{\cdot}{2})$ as ϕ_2, and compute the two-scale symbols $\widetilde{P}_{A_1}(\mathbf{z})$ and $\widetilde{P}_{2I_2}(\mathbf{z})$ of $\widetilde{\Phi}^b := [\phi_1, \phi_1(\frac{\cdot}{2})]^T$, with dilation matrices A_1 and $2I_2$, respectively. This can be achieved simply by observing that $\widehat{\phi_1(\frac{\cdot}{2})} = 4\widehat{\phi_1}(2\omega)$ and applying (28) to obtain

$$\widehat{\widetilde{\Phi}^b}(\omega) = \frac{1}{8}\begin{bmatrix} 8 & 0 \\ p(\mathbf{z}) - 1 & 9 \end{bmatrix}\widehat{\Phi^b}(\omega),$$

which immediately yields:

$$\widetilde{P}_{A_1}(\mathbf{z}) = \frac{1}{72}\begin{bmatrix} 8 & 0 \\ p(e^{-iA_1^T\omega}) - 1 & 9 \end{bmatrix}P_{A_1}(\mathbf{z})\begin{bmatrix} 9 & 0 \\ 1 - p(\mathbf{z}) & 8 \end{bmatrix},$$

and

$$\widetilde{P}_{2I_2}(\mathbf{z}) = \frac{1}{72}\begin{bmatrix} 8 & 0 \\ p(e^{-i2\omega}) - 1 & 9 \end{bmatrix}P_{2I_2}(\mathbf{z})\begin{bmatrix} 9 & 0 \\ 1 - p(\mathbf{z}) & 8 \end{bmatrix}.$$

References

[1] C.K. CHUI, *Multivariate Splines*, NSF-CBMS Series #54, SIAM, Philadelphia, 1988.

[2] C.K. Chui, Vertex splines and their applications to interpolation of discrete data, In: *Computation of Curves and Surfaces*, W. Dahmen, M. Gasca and C.A. Micchelli (eds.), Kluwer Academic, 1990, pp. 137–181.

[3] C.K. Chui, H.C. Chui, and T.X. He, Shape-preserving interpolation by bivariate C^1 quadratic splines, In: *Workshop on Computational Geometry*, A. Conte, V. Demichelis, F. Fontanella and I. Galligani (eds.), World Sci. Publ. Co., Singapore, 1992, pp. 21–75.

[4] N. Dyn, D. Levin, and J.A. Gregory, A butterfly subdivision scheme for surface interpolation with tension control, *ACM Trans. Graphics* **2** (1990), 160–169.

[5] R.A. Haddad, A.N. Akansu, and A. Benyassine, Time-frequency localization in transforms, subbands, and wavelet: a critical review, *Opti. Eng.* **32** (1993), 1411–1429.

[6] B. Han and Q.T. Jiang, Multiwavelets on the interval, *Appl. Comput. Harmon. Anal.* **12** (2002), 100–127.

[7] B. Han, T. Yu, and B. Piper, Multivariate refinable Hermite interpolants, Math. Comp., to appear.

[8] P.N. Heller, H.L. Resnikoff, and R.O. Wells, Wavelet matrices and the representation of discrete functions, In: *Wavelets-A Tutorial in Theory and Applications*, C.K. Chui (ed.), Academic Press, Boston, MA, 1992, pp. 15–50.

[9] R.Q. Jia, Shift-invariant spaces and linear operator equations, *Israel J. Math.* **103** (1998), 259–288.

[10] R.Q. Jia and Q.T. Jiang, Approximation power of refinable vectors of functions, In: *Wavelet analysis and applications*, Studies Adv. Math. #25, Amer. Math. Soc., Providence, RI, 2002, pp. 155–178.

[11] R.Q. Jia and C.A. Micchelli, Using the refinement equations for the construction of pre-wavelets II: Powers of two, In: *Curves and surfaces*, Academic Press, Boston, MA, 1991, pp. 209–246.

[12] Q.T. Jiang and P. Oswald, Triangular $\sqrt{3}$-subdivision schemes: the regular case, *J. Comp. Appl. Math.* **156** (2003), 47–75.

[13] Q.T. Jiang, P. Oswald, and S.D. Riemenschneider, $\sqrt{3}$-subdivision schemes: maximal sum rule orders, *Constr. Approx.* **19** (2003), 437–463.

[14] L. Kobbelt, $\sqrt{3}$-subdivision, In: *Computer Graphics Proceedings*, Annual Conference Series, July 2000, pp. 103–112.

[15] U. Labsik and G. Greiner, Interpolatory $\sqrt{3}$-subdivision, *Proceedings of Eurographics 2000, Computer Graphics Forum*, vol. 19, 2000, pp. 131–138.

[16] C. Loop, Smooth subdivision surfaces based on triangles, Master's thesis, Dept. of Math., University of Utah, 1987.

[17] P. Oswald and P. Schröder, Composite primal/dual $\sqrt{3}$-subdivision schemes, *CAGD* **20** (2003), 135–164.

[18] D. Pollen, $SU_I(2, F[z, 1/z])$ for F a subfield of C, *J. Amer. Math. Soc.* **3** (1990), 611–624.

[19] P.P. Vaidyanathan, T.Q. Nguyen, Z. Doganata, and T. Saramäki, Improved technique for design of perfect reconstruction FIR QMF banks with lossless polyphase matrices, *IEEE Trans. ASSP* **37** (1989), 1042–1056.